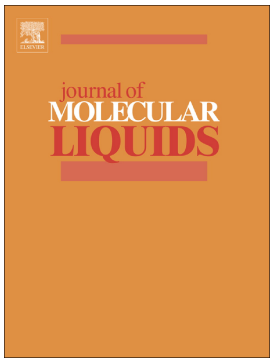

para'Xylyl bis'1'methylimidazolium bis(trifluoromethanesulfonyl)imide: Synthesis, crystal structure, thermal stability, vibrational studies

Boumediene Haddad, Annalisa Paolone, Didier Villemin, Jean-François Lohier, Mokhtar Drai, Serge Bresson, Ouissam Abbas, El-habib Belarbi

PII: S0167-7322(18)30307-6
DOI: doi:10.1016/j.molliq.2018.03.113
Reference: MOLLIQ 8887

To appear in: *Journal of Molecular Liquids*

Received date: 22 January 2018
Revised date: 15 March 2018
Accepted date: 27 March 2018

Please cite this article as: Boumediene Haddad, Annalisa Paolone, Didier Villemin, Jean-François Lohier, Mokhtar Drai, Serge Bresson, Ouissam Abbas, El-habib Belarbi , para'Xylyl bis'1'methylimidazolium bis(trifluoromethanesulfonyl)imide: Synthesis, crystal structure, thermal stability, vibrational studies. The address for the corresponding author was captured as affiliation for all authors. Please check if appropriate. Molliq(2017), doi:10.1016/j.molliq.2018.03.113

Para-xylyl bis-1-methylimidazolium bis(trifluoromethanesulfonyl)imide: synthesis, crystal structure, thermal stability, vibrational studies.

Boumediene Haddad [1,2,3], Annalisa Paolone [4], Didier Villemin [3], Jean-François Lohier [3], Mokhtar Drai [2,5], Serge Bresson [6], Ouissam Abbas [7], El-habib Belarbi [2]

[1] Department of Chemistry, Dr Moulay Tahar University of Saida, Saida, Algeria
[2] Synthesis and Catalysis Laboratory LSCT, Tiaret University, Tiaret, Algeria
[3] LCMT, ENSICAEN, UMR 6507 CNRS, University of Caen, 6 bd Ml Juin, 14050 Caen, France
[4] CNR-ISC, U.O.S. La Sapienza, Piazzale A. Moro 5, 00185 Roma, Italy
[5] Université Djillali Liabes, BP 89, 22000 Sidi-Bel-Abbes, Algeria
[6] Laboratoire de Physique des Systèmes Complexes, Université Picardie Jules Verne, 33 rue St Leu, 80039 Amiens cedex, France.
[7] Centre Wallon de Recherche Agronomique, CRA-W, Bâtiment Maurice Henseval, Chaussée de Namur, 24, 50030 Gembloux, Belgium.

ABSTRACT

In this study, a new para-xylyl linked di-imidazolium [p-$C_6H_4(CH_2ImMe)_2^+$] ionic liquid (DIL) containing the bis(trifluoromethanesulfonyl)imide [$(CF_3SO_2)_2N^-$] anion is synthesized. The method is based on the alkylation reaction of 1-methyl imidazole, followed by anion exchange. The obtained DIL is characterized by ^{1}H-NMR, ^{13}C-NMR, ^{19}F-NMR and FT-IR spectroscopy. The melting point and the subsequent decomposition of [p-$C_6H_4(CH_2ImMe)_2^+$][$(CF_3SO_2)_2N^-$]$_2$ are measured by using differential scanning calorimetry (DSC) and thermogravimetric (TGA) analyses in the temperature range from 25 to 700 °C. Thermal analysis indicated that this DIL melted below 100 °C and can, therefore, be classified as an ionic liquid. Vibrational spectroscopy studies were conducted by infrared (IR), Raman (FT-Raman) spectroscopy and DFT calculations. Moreover, the crystal structure is investigated by single crystal X-ray diffraction (XRD) method. The X-ray studies on [p-$C_6H_4(CH_2ImMe)_2^+$][$(CF_3SO_2)_2N^-$]$_2$ show that it crystallizes in the monoclinic system with space group P21/c. The theoretical structural parameters such as bond lengths, bond angles and dihedral angles determined by DFT methods are in good agreement with the XRD results.

KEYWORDS: di-imidazolium; bis(trifluoromethanesulfonyl)imide; para-xylyl; crystal structure; vibrational spectra; thermal stability; Raman measurements; DFT.

1. INTRODUCTION

During the last decade, the chemistry of ionic liquids has garnered spectacular interest from the scientific community. Due to their industrial accessibility and their tunable physico-chemical properties [1], these fascinating fluids have been a highly active field of research in many applications.

At the laboratory level, the chemical reaction of the precursors as imidazole [2], phosphine [3], piperidine [4] or pyrrolidine [5] with alkyl halides yields transfer of the alkyl group to the precursor ring and results in halogenides ionic liquids. Unfortunately, the range of obtained ionic liquids during this step is limited and it is not of primary concern for applications.

The reaction of halogenides ionic liquids with different bulk anions opens a wide range of opportunity for obtaining new ionic liquids with special properties [6-7]. The list of the resulting ionic liquids includes bis(trifluoromethylsulfonyl)imide [8], nitrate [9], alkyl sulphates [10], dicyanamide [11], thiocynate [12], trifluoromethanesulfate [13], tetrafluoroborate [14], and hexafluorophosphate [15]. Moreover, the possibility of functionalization of imidazole precursor opens up even a wider opportunity for obtaining new functionalized ionic liquid with different properties [16].

Quite recently, a great deal of interest has taken place in the synthesis of a new category of ILs, namely dicationic ionic liquids (DILs) [17]. Compared to traditional monocationic ILs, dicationic liquids are more tunable. Moreover, the large number of possible change in cation, anion or in side chain (linker) resulted into two head groups linked by a rigid or flexible spacer and two monoanions [18].

Compared to their monocationic counterparts, DILs usually display a higher thermal stability: their thermal decomposition temperatures range from 330 °C up to 400°C, while they can be as low as 145-185°C for monocationic ILs.[17-19] Also the viscosity of DILs is higher than that of usual ionic liquid [19]. Moreover, the viscosity of DILs can be tuned by varying the length of the chain linking the anions: the longer the chain, the higher the viscosity.[19] These properties can be used in a combined way in applications concerning lubrification at high temperature.[19] DILs have found also application as agent for the extraction of phenolic compounds from oil mixtures [17], as surfactant [20] or as catalysts for the esterification reaction [18,21].

Despite the wealth of papers on dicationic ionic liquids and their applications [20-23], there are a few experimental and computational studies on these compounds to understand their structure-property relationships and vibrational spectra [18, 24-27].

In this paper, a new para-xylyl linked di-imidazolium Ionic Liquid (DIL) containing the bis(trifluoromethanesulfonyl)imide [$(CF_3SO_2)_2N^-$] was prepared and characterized by ^{1}H-NMR, ^{13}C-NMR, ^{19}F-NMR spectroscopy. Its structure was also determined by a single-crystal X-ray diffraction. Moreover, the thermal stability of [p-

$C_6H_4(CH_2ImMe)_2^+][(CF_3SO_2)_2N^-]_2$ and its decomposition process were investigated. Furthermore, the relationship between the structure and the melting point is discussed.

Additionally, the vibrational behaviour of $[p\text{-}C_6H_4(CH_2ImMe)_2^+][(CF_3SO_2)_2N^-]_2$ was investigated by measuring the infrared (IR) and Raman spectra and by a comparison with calculations based on the Density Functional Theory (DFT).

2. EXPERIMENTAL

2.1 Materials, synthesis, and characterization

The reagents used in this study, 1-methyl-1H-imidazole (>99%), α,α′-dichloro-p-xylène (98%), lithium bis(trifluoromethylsulfonyl) Imide (99%), diethyl ether and N,N-dimethylformamide were purchased from Aldrich and used as received. Deionized H_2O was obtained with a Millipore ion-exchange resin deionizer.

The synthetic route used to prepare the α,α′ diimidazolium-p-xylene dichloride DIL described herein is depicted in Scheme 1. Briefly, the $[p\text{-}C_6H_4(CH_2ImMe)_2][Cl]_2$ was prepared in high yield (93%) from 1-methylimidazole (4.26 g, 40 mmol) and the p-xylylene dichloride (2.27 g, 10 mmol) by slight modifications of the procedures reported in the literature [28-29].

$[p\text{-}C_6H_4(CH_2ImMe)_2^+][(CF_3SO_2)_2N^-]_2$ was prepared by an anion exchange reaction from Cl^- to $[(CF_3SO_2)_2N^-]$ which was carried out by mixing $[p\text{-}C_6H_4(CH_2ImMe)_2^+][Cl^-]_2$ and lithium bis(trifluoromethylsulfonyl) Imide (molar rate = 1:1) in 20 mL of distilled water at room temperature for 2 h. Two phases appeared; the lower phase was the ionic liquid; it was washed with water (2x10 mL) and then recovered after ten minutes of centrifugation (3000 rpm). Aspect: white solid, yield: 95 %, mp: 65 °C.

In order to obtain high purity, the obtained DIL was dried in a high-vacuum line ($p<10^{-5}$ bar) for 4 days at approximately 40°C. Finally, the water content was below 150 ppm in $[p\text{-}C_6H_4(CH_2ImMe)_2][Cl]_2$ and below 350 ppm in $[p\text{-}C_6H_4(CH_2ImMe)_2^+][(CF_3SO_2)_2N^-]_2$; this measure was carried out by coulometric Karl Fischer titration performed by means of a Metrohm 831.

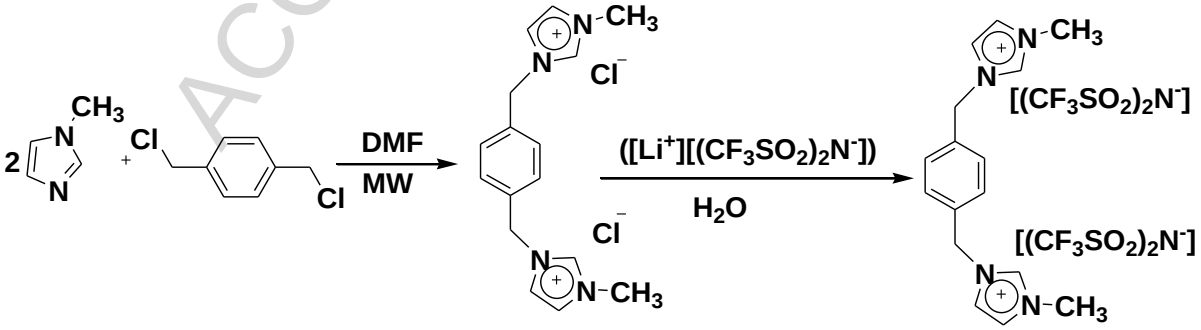

Scheme 1. General synthesis of $[p\text{-}C_6H_4(CH_2ImMe)_2][(CF_3SO_2)_2N^-]_2$, MW = microwave.

^{1}H-NMR (500 MHz), ^{13}C-NMR (125.75 MHz) and ^{19}F-NMR (470.62 MHz) spectra were recorded on a Bruker DRX 500 MHz spectrometer. Spectra were recorded in

dimethylsulfoxide (DMSO-d_6), using the DMSO residual peak as the ^1H internal reference (δ = 2.5 and 3.3), and the central peak of DMSO-d_6 at δ = 39.5 for the ^{13}C reference. Chemical shifts (δ) are given in ppm and referred to the internal solvent signal, namely TMS and $CFCl_3$, respectively. Preliminary IR spectra were recorded on a FT-IR Perkin-Elmer Spectrum BX spectrophotometer with a resolution of 4 cm^{-1} in the range 4000-650 cm^{-1} in order to check the occurrence of the expected chemical reactions and the production of the DIL (see Section 4.1). Afterwards, IR absorbance spectra were collected with a better resolution as described in Section 2.4 for comparison with DFT calculations (reported in Section 4.3).

2.2 X-ray Diffraction

The single crystal of $[p\text{-}C_6H_4(CH_2ImMe)_2^+][(CF_3SO_2)_2N^-]_2$ available for the X-ray single-crystal determination can be easily obtained by recrystallization from a mixed chloroform/acetonitrile (1:1) system. Single crystal structure was determined at 293 K by a Bruker-Nonius Kappa CCD area detector diffractometer with graphite monochromatized Mo$K\alpha$ radiation (λ= 0.71073 Å). Moreover, the powder X-ray diffraction (XRD) pattern was collected on a Rigaku Miniflex 600 X-Ray Diffractometer using Ni filtered Cu Kα radiation (λ =1.54056 Å) in the 2θ range 5-50º with a step size of 0.02º at room temperature. The programs for structure solution and refinement were SHELXS-97 [30] and SHELXL-2014 [31], respectively.

2.3 FT-Raman measurements

The FT-RAMAN spectrum was acquired on a Vertex 70-RAM II Bruker FT-Raman spectrometer. This instrument is equipped with a Nd:YAG laser (yttrium aluminium garnet crystal doped with triply ionized neodymium) with a wavelength of 1064 nm and a maximum power of 1.5 W. The measurement accessory is pre-aligned: only the Z-axis of the scattered light is adjusted to set the sample in the appropriate position regarding the local measurement point. The RAM II spectrometer is equipped with a liquid nitrogen cooled Ge detector. FT-Raman spectra [45-4000cm^{-1}] were collected with 1 cm^{-1} resolution by co-adding 128 scans for each spectrum at room temperature. The OPUS 6.0 software was used for the spectral acquisition, manipulation and transformation. These measurements were performed in the Walloon Agricultural Research Center (Craw) Belgium.

2.4 IR measurements

The absorbance spectrum of $[p\text{-}C_6H_4(CH_2ImMe)_2^+][(CF_3SO_2)_2N^-]_2$ was measured by means of an Agilent Cary 660 spectrometer equipped with a ceramic source, a DTGS detector and a KBr beamsplitter. A few mg of powder were dissolved in KBr powder in a mass ratio of 3:100 and pressed in a dye in order to obtain a self standing pellet.

2.5 Thermal measurements

Concomitant thermogravimetric analysis (TG) and differential scanning calorimetric (DSC) measurements were performed by means of a Setaram Setsys Evolution 1200 TG System. In

the experiment an initial mass of ~15 mg was used; the heating temperature was fixed at 5 °C/min under a dynamical helium atmosphere with a flux of 60 ml/min.

3. COMPUTATIONAL

The isolated [p-$C_6H_4(CH_2ImMe)_2^+$] and [$(CF_3SO_2)_2N^-$] ions composing the studied DIL were investigated computationally by means of the Spartan software [32-33]. The structure of the relevant ions (*trans*- and *cis*-[$(CF_3SO_2)_2N^-$] and *trans*- and *cis*-[p-$C_6H_4(CH_2ImMe)_2^+$]) was determined by the minimization of energy, using DFT calculations at the B3LYP level of theory with a 6-31G** basis set. This basis set has been largely utilized for determining the structure and the vibrational properties of a large number of ionic liquids [34-36].
Both the Raman and the IR spectra of each ion were simulated by summing Gaussian curves centered at each calculated vibrational frequency with a fixed 10 cm^{-1} peak width.

4. RESULTS AND DISCUSSION

4.1 NMR results

The structures of synthesized DILs are confirmed by using ^1H, ^{13}C, ^{19}F-NMR and FT-IR spectroscopy, in order to check the occurrence of the expected chemical reactions and confirm the absence of any impurities. The spectroscopic data are given below and the H and C atom labeling and the corresponding ^1H, ^{13}C and ^{19}F-NMR spectra are shown in Fig. 1(a, b and c).

3,3'-dimethyl-1,1'-(1,4-phenylenedimethylene)-di(1H-imidazolium) dichloride:
[p-$C_6H_4(CH_2ImMe)_2^+$] 2[Cl^-]:
^{1}H-NMR (DMSO-d_6) δ_H (ppm) : 9.48 (s, NCHN, 2H), 7.85 (s, NCHC, 2H), 7.74 (s, NCHC, 2H), 7.51 (s, -C_6H_4-, 4H), 5.47 (s, -CH_2-, 4H), 3.86 (s, 2×CH_3, 6H);
^{13}C-NMR (DMSO-d_6) δ ppm: 36.26, 51.58, 122.54, 124.46, 129.19, 135.85, 137.22;
IR ($\tilde{\nu}$/cm^{-1}): 3032 [ν(=C-H)$_{Arom}$], 2874[ν (C–H)], 1560[ν(C=C)], 1442 [δ(C-H)], 1081 [ν(C-N)], 742 [ν(C-H)].

3,3'-dimethyl-1,1'-(1,4-phenylenedimethylene)-di(1H-imidazolium) di(bis(trifluoromethylsulfonyl) Imide):[p-$C_6H_4(CH_2ImMe)_2^+$][$(CF_3SO_2)_2N^-$]$_2$:
^{1}H-NMR (DMSO-d_6) δ_H (ppm) : 9.20 (s, NCHN, 2H), 7.75 (s, NCHC, 2H), 7.71 (s, NCHC, 2H), 7.46 (s, -C_6H_4-, 4H), 5.42 (s, -CH_2-, 4H), 3.85 (s, 2×CH_3, 6H);
^{13}C-NMR (DMSO-d_6) δ ppm: 36.46, 51.78, 118.51, 120.97, 122.53, 124.50, 129.19, 135.65, 136.95.
^{19}F-NMR (DMSO-d_6) δ_F (ppm): -78.94 (s, [$(CF_3SO_2)_2N^-$]).
IR ($\tilde{\nu}$/cm^{-1}): 3150-3200 [ν(=C-H)$_{Arom}$], 2892 [ν (C–H)], 1630 [(C=N)], 1540 (C–C), 1510[ν(C=C)], 1442 [δ(C-H)], 1200[(S-O)], 1081 [ν(C-N)], 710 [ν(C-H)].

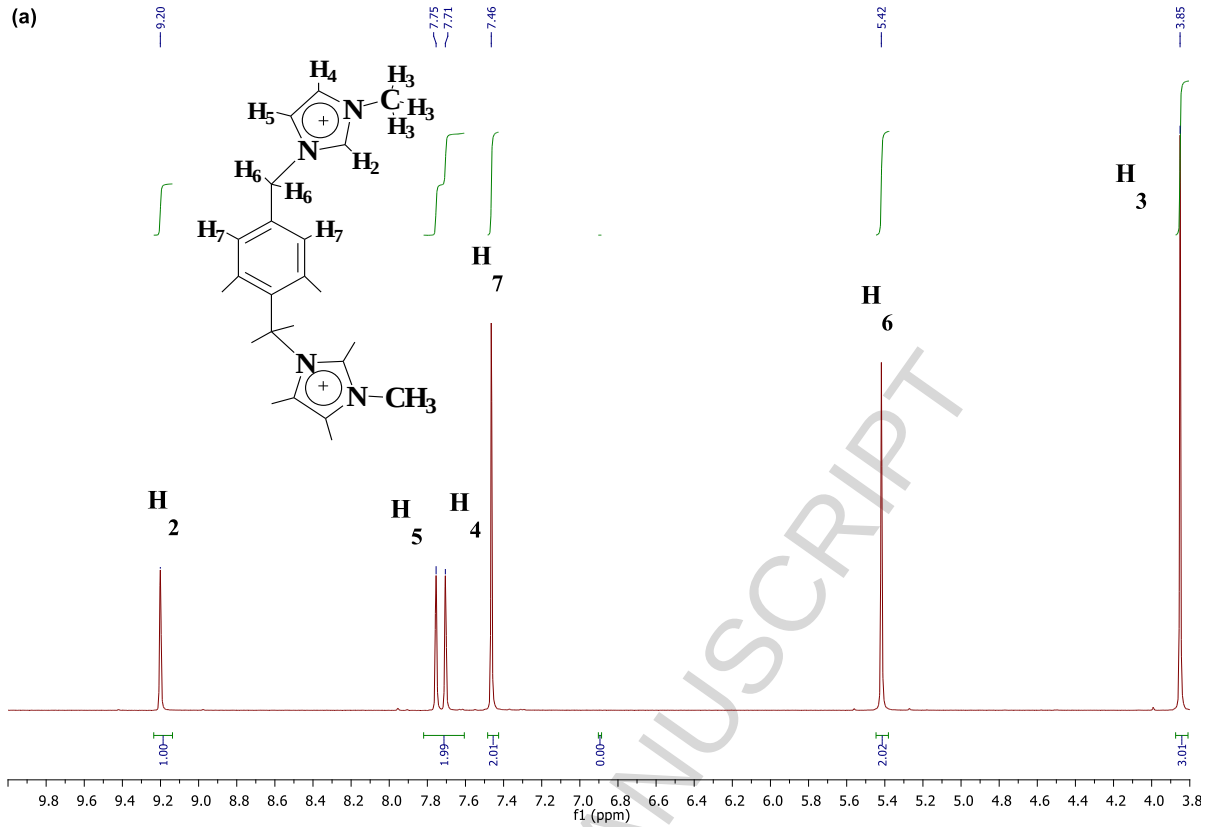

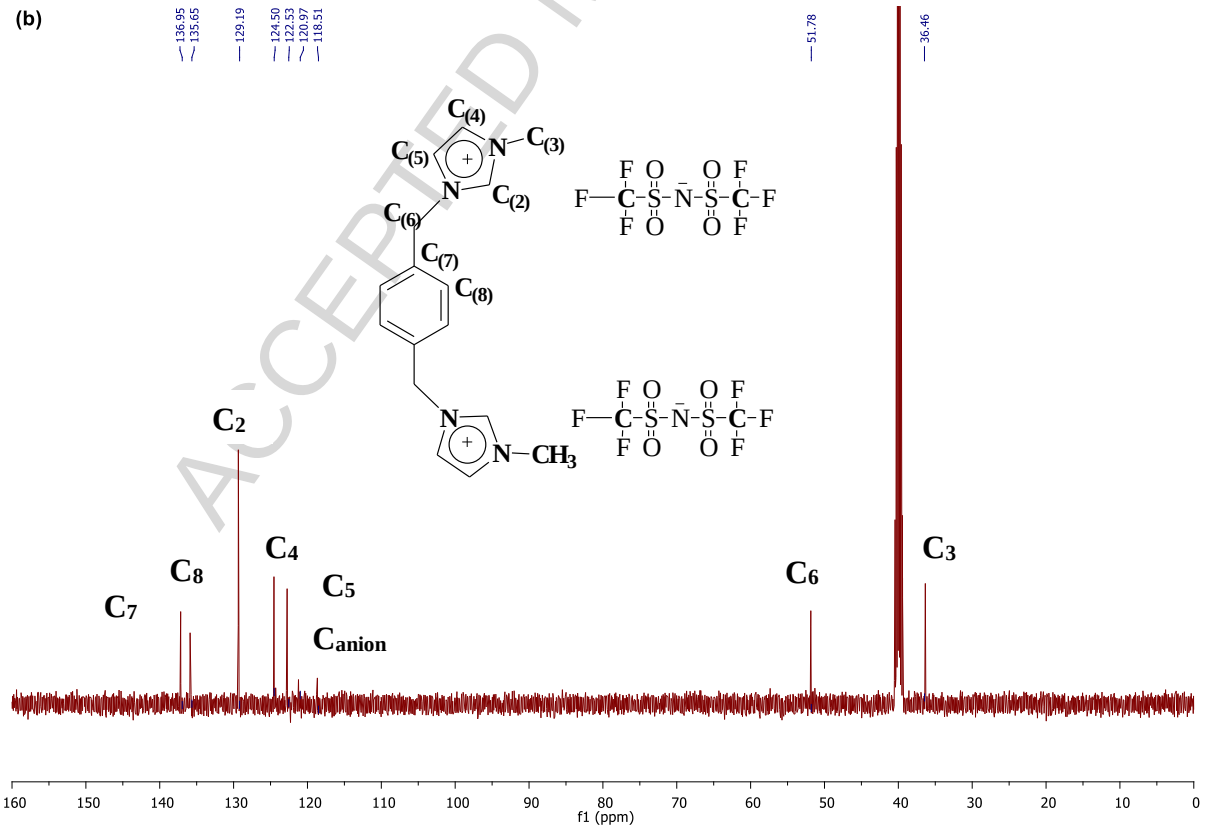

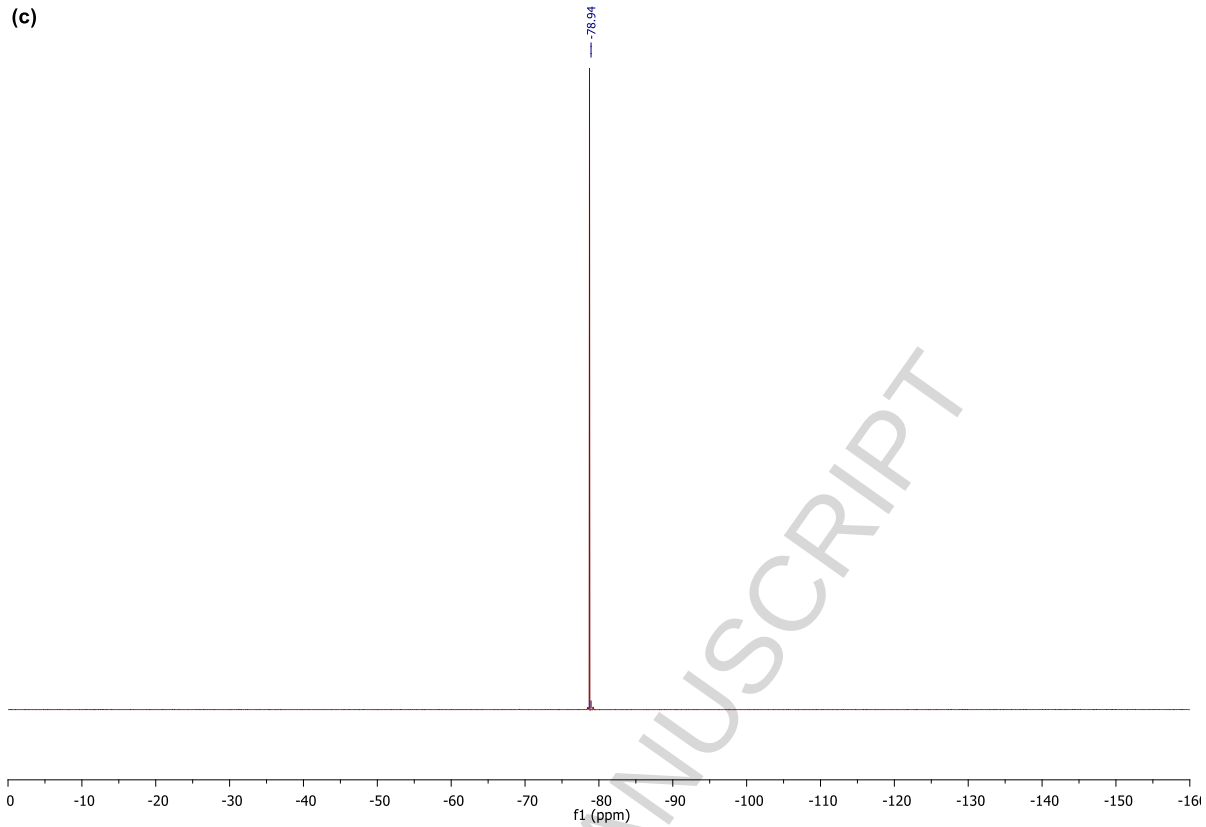

Figure 1. Hydrogen atom labeling and ^{1}H NMR (500 MHz) (a), carbon atom labeling and ^{13}C NMR (125.75 MHz) (b) and ^{19}F NMR (470.62 MHz) (c) of [p-$C_6H_4(CH_2ImMe)_2^+$][$(CF_3SO_2)_2N^-$]$_2$

4.1 Thermal analysis

The results of the thermogravimetric analysis of [p-$C_6H_4(CH_2ImMe)_2^+$][$(CF_3SO_2)_2N^-$]$_2$ are shown in Figs. 2 (a and b). Upon heating, we observed that the thermal decomposition occurs in the temperature range ≈ 400–500 °C, with a mass loss that reaches 85% at 485 °C. The corresponding DSC signal shows two endothermic peaks, the first one (around 65 °C) can be assigned to the melting process and, therefore, the DIL can be categorised as a room-temperature ionic liquid [37]. The second peak can be attributed to the thermal decomposition. Differently from Ibrahim el al [38], this DIL has a lower melting point compared to the same cation [p-$C_6H_4(CH_2ImMe)_2^+$] with dibromide anion, mp : 245–247 °C; di(tetrafluoroborate), mp : 225–228 °C; di(hexafluorophosphate), mp: 213 °C and with triflate anion with melting point equal to 155–157 °C. Indeed, this difference in melting points is due to related cation–anion interaction type. Following the work of Weingärtner [39], an increase in size, anisotropy, and internal flexibility of the ions should lower the melting temperature. Furthermore, as reported by Wilkes in 2002 [40], the ionic liquids with large cations and large anions should have even lower melting points, which is exactly what is observed in our DIL case. As [p-$C_6H_4(CH_2ImMe)_2^+$] cation is bulky, its charge is not localized: it generates few interactions with [$(CF_3SO_2)_2N^-$] anion, which lower the melting point of the obtained ionic liquid.

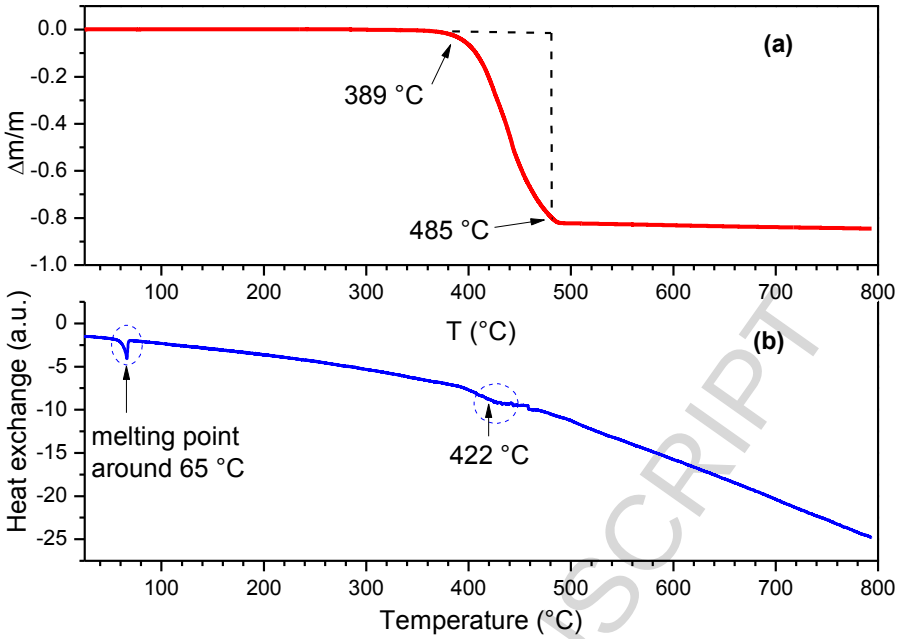

Figure 2. The TG (a) and DSC (b) curves of $[p\text{-}C_6H_4(CH_2ImMe)_2^+][(CF_3SO_2)_2N^-]_2$.

4.2 Experimental X-ray diffraction results and comparison with computational results

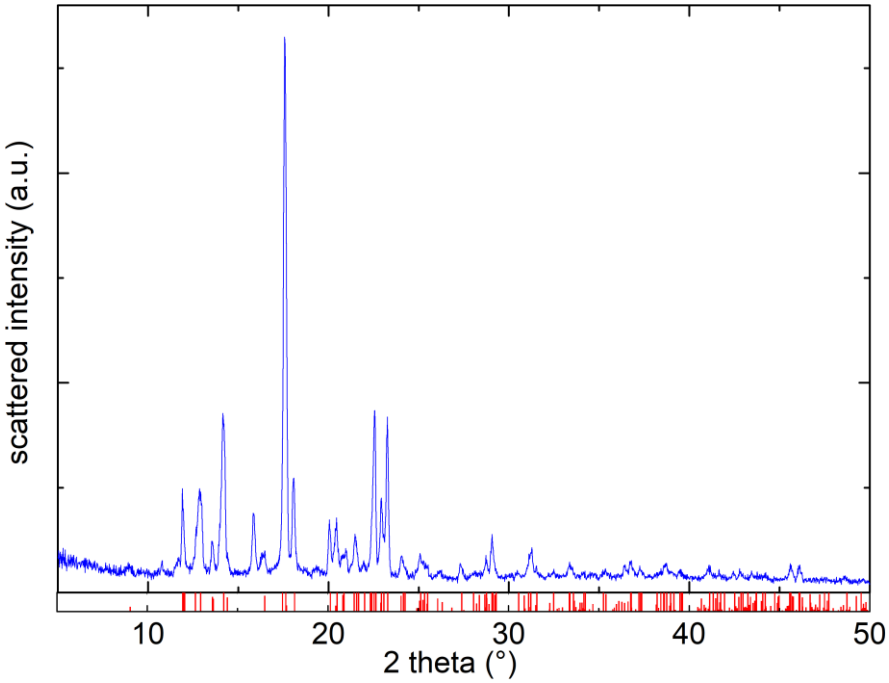

Figure 3. Powder X-ray diffraction pattern of $[p\text{-}C_6H_4(CH_2ImMe)_2^+][(CF_3SO_2)_2N^-]_2$.

The powder XRD pattern of [p-$C_6H_4(CH_2ImMe)_2^+$][$(CF_3SO_2)_2N^-$]$_2$ is shown in Fig. 3. It shows many fine and quite intense peaks, which indicate a good crystallinity of our DIL.
The structure of the [p-$C_6H_4(CH_2ImMe)_2^+$][$(CF_3SO_2)_2N^-$]$_2$ is shown in Fig. 4. Crystal structure is deposited in Cambridge Crystallographic Data Centre as supplementary publication number CCDC-**1815473** and can be freely accessed at www.ccdc.cam.ac.uk. A summary of the crystal data obtained from single crystal diffraction data of [p-$C_6H_4(CH_2ImMe)_2^+$][$(CF_3SO_2)_2N^-$]$_2$ is presented in Table 1.

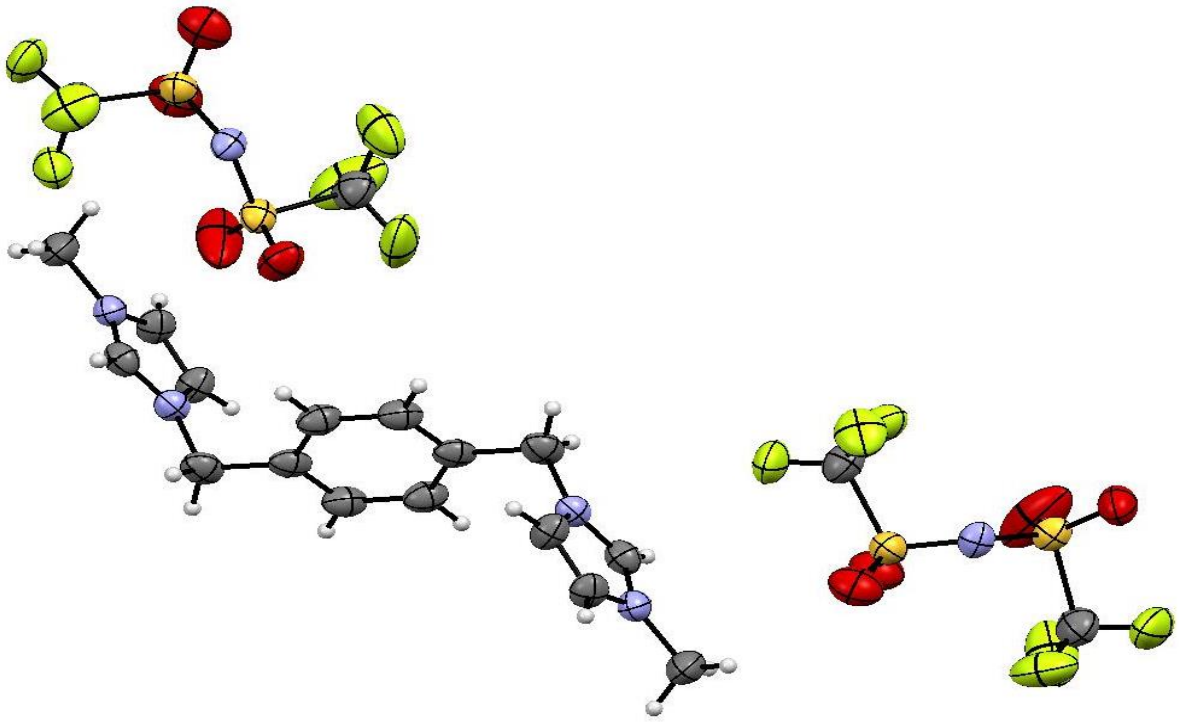

Figure 4. A view of the molecular structure of [p-$C_6H_4(CH_2ImMe)_2$][$(CF_3SO_2)_2N^-$]$_2$ with ellipsoids shown at the 30% probability level.

Table 1. Crystallographic data for [p-$C_6H_4(CH_2ImMe)_2^+$][$(CF_3SO_2)_2N^-$]$_2$.

Compound	[p-$C_6H_4(CH_2ImMe)_2^+$][$(CF_3SO_2)_2N^-$]$_2$
CCDC no.	1815473
Empirical formula	$C_{26}H_{32}O_8N_6F_{12}S_4$
Formula weight	828.65
Temperature /K	291
Wavelength /Å	0.71073
Crystal system	monoclinic
Space group	P 2_1/n
Unit cell dimensions /Å,°	a =8.68540 (10) Å b =13.6572(2) Å c =13.9674(2)Å α = 90° β = 90.328(10) ° γ = 90°
Volume /Å^3	1656.76 Å^3
Z	4
Crystal size /mm^3	0.30 x 0.25 x 0.21

Goodness-of-fit on *F*2	1.05
Final *R* indices [*I* - 2σ(*I*)]	*R*1 = 0.075
R indices (all data)	*wR*2 = 0.264

This DIL crystallizes in the monoclinic system, space group P 2_1/n; the unit cell parameters determined at 291 K are: a =8.68540 (10) Å, b =13.6572(2) Å, c =13.9674(2)Å, α = 90°, β = 90.328(10) °, γ = 90°, Cell volume: 1656.76 $Å^3$, Z = 4.

A combination of experimental X-ray diffraction and DFT calculation is necessary to localize the interactions between anions and cations and explore conformational stability at molecular level. The possible geometry of [p-$C_6H_4(CH_2ImMe)_2^+$] and [$(CF_3SO_2)_2N^-$]$_2$ molecular crystal is optimised by B3LYP method using 6-31G** basis set and is presented in Fig. 5. The calculated optimised geometrical parameters namely bond lengths, bond angles and selected dihedral angles are listed in Table 2.

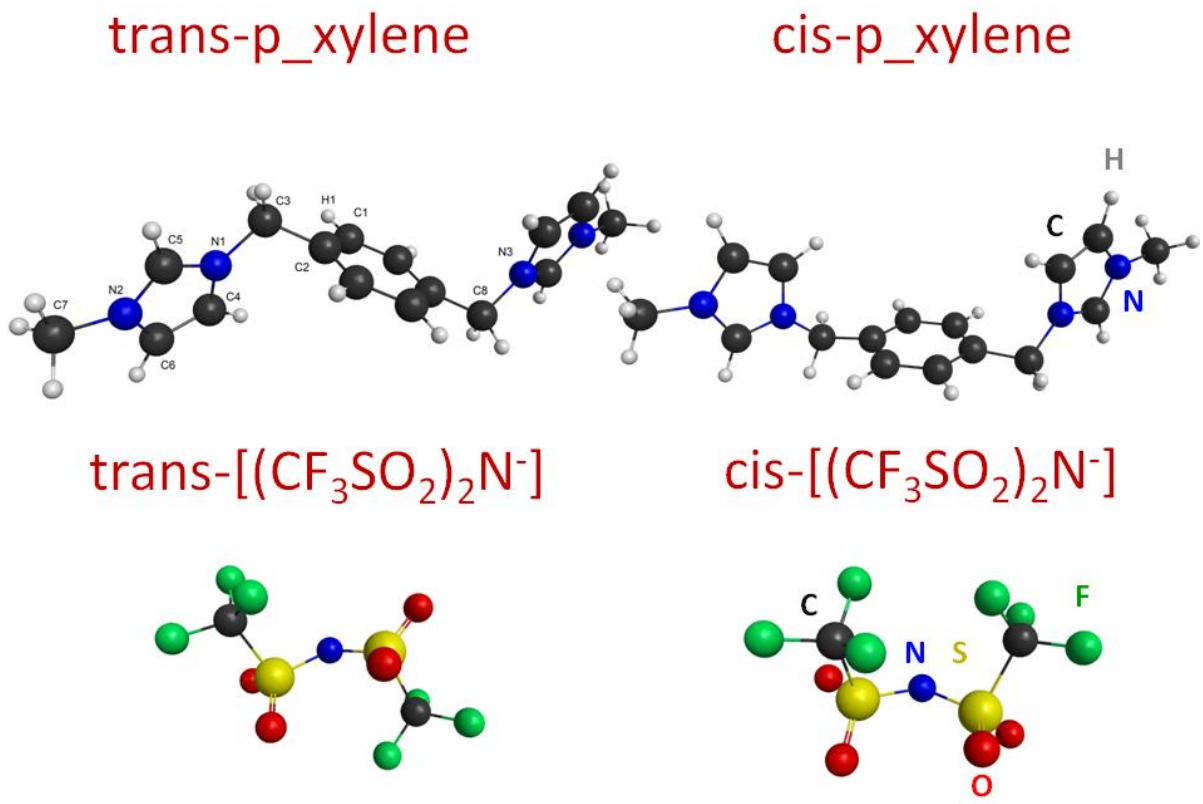

Figure 5. Schematic view of the possible geometries of the ions composing the ionic liquid.

Analyses of the experimental bond lengths and angles clearly show that the two imidazolium rings in [p-$C_6H_4(CH_2ImMe)_2^+$] cation are placed on the opposite sides of the p-xylene plane in a transoid configurations with N-C-C-N torsion angle = 180 °, which, according to DFT calculations, has the minimum energy between the two investigated conformers. The same conformation of the imidazolium rings have been reported for other fluorinated imidazolium salts, namely the 3,3'-dimethyl-1,1'-(1,4-phenylenedimethylene)-di(1H-imidazolium) DILs

containing the bis(tetrafluoroborate), bis(hexafluorophosphate) or the bis (triflate) anions [38, 41].

Table 2 reports a comparison of the significative interatomic distances obtained by means of X-Ray diffraction of $[p\text{-}C_6H_4(CH_2ImMe)_2^+][(CF_3SO_2)_2N^-]_2$ with the results of the present computational study. One can observe that the bond lengths and bond angles are generally in good agreement between the calculated distances and angles and the X-Ray experimental ones.

Table 2. Comparison of significative bond lengths (in Å) and angles (in degrees) of the α,α′ diimidazolium-p-xylene ion obtained by a computationally study or by XRD experimentally.

	Trans-p_xylene (DFT calculations)	Cis-pxylene (DFT calculations)	XRD results
Bond lengths (Å)			
C1-C2	1.39	1.40	1.377(6)
C1-H1	1.09	1.09	0.930
C2-C3	1.52	1.52	1.493(4)
C3-N1	1.49	1.48	1.475(4)
N1-C4	1.38	1.38	1.365(4)
N1-C5	1.34	1.34	1.311(4)
C4-C6	1.36	1.36	1.339(5)
N2-C7	1.47	1.47	1.469(5)
Angles (degrees)			
N1-C3-C2	113.24	114.16	111.8(3)
N1-C3-C8-N3	179.72	77.39	180

Upon close inspection of the experimental results by means of XRD diffraction, the $[(CF_3SO_2)_2N^-]$ anion show a Trans conformation with S–N–S bond angle, 128.62°; and C–S-----S–C torsion angle = 168.12°,(-CF_3 groups locate on the opposite sides of the plane defined by the S−N−S bonds); indeed, the trans conformer is more stable than the *cis* one due to the bulky -CF_3 group, following the results of Holbrey and coworkers [42].

We noticed that the S–O bond length falls in the range 1.31(2)-1.433(9) A° and the O−S−O angles fall in the range 122.0(8)°-119.5(6)°. Symmetry code : $^{(a)}$x,y,z ; $^{(b)}$1/2-x,1/2+y,1/2-z ;$^{(c)}$ -x,-y,-z ; $^{(d)}$1/2+x,1/2-y,1/2+z.

As shown by Fig. 6, XRD results indicate that in the asymmetric unit, the [p-$C_3H_4(CH_2ImMe)$] cation and $[(CF_3SO_2)_2N^-]$ anions are related through four bonding interactions as shown by dashed lines. Two H-bonds occur between the hydrogen of methylene group (-CH_2-), as proton donors, to $[(CF_3SO_2)_2N^-]$ oxygen, that acts as proton acceptors atom. Their distances are (F……$H_{methylene}$ =2.446Å) and (F……$H_{methylene}$ =2.559Å), respectively.

Furthermore, the $[(CF_3SO_2)_2N^-]$ anion participates also by the oxygen atoms of -SO_2 moieties as proton acceptors and the acidic imidazolium C(2)–H as proton donors with the distances (C(2)–H …….O =3.129 Å). Finally, one hydrogen-bonding contact between the hydrogen

attached directly to the imidazolium ring C(4)–H and N atom of $[(CF_3SO_2)_2N^-]$ anion with (C(4)–H …….N =2.563 Å).

According to Levason and co-workers [43] and Panda et al [44], all these four contacts can be classified as weak hydrogen bonds since their distances are higher than 2.3 Å.

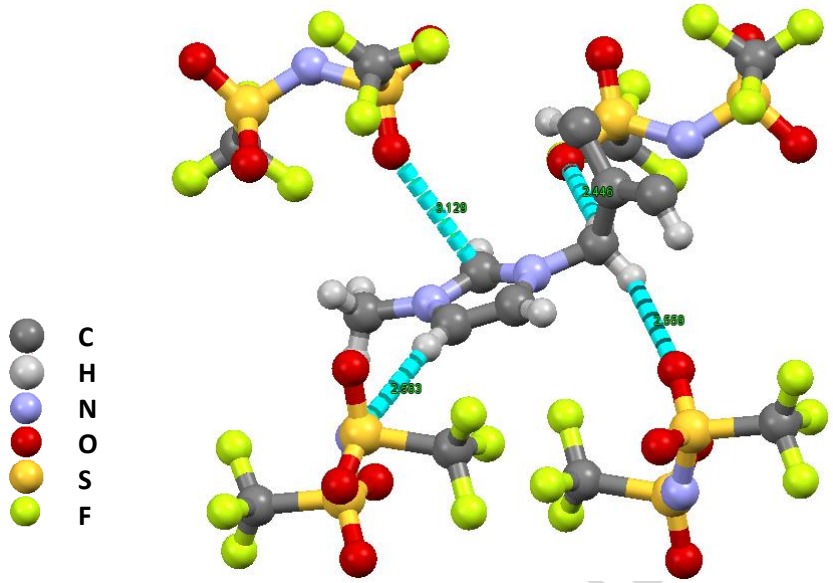

Figure 6. Hydrogen bonding surrounding each cation in the crystal of $[p\text{-}C_6H_4(CH_2ImMe)_2^+][(CF_3SO_2)_2N^-]_2$.

The packing diagram of the investigated DIL is presented in Fig. 7. When viewed along the *a* axis, the packing comprises of $[p\text{-}C_6H_4(CH_2ImMe)_2^+]$ cation forming Z-shaped zigzag patterns in layers around rows of the counter anions $[(CF_3SO_2)_2N^-]$.

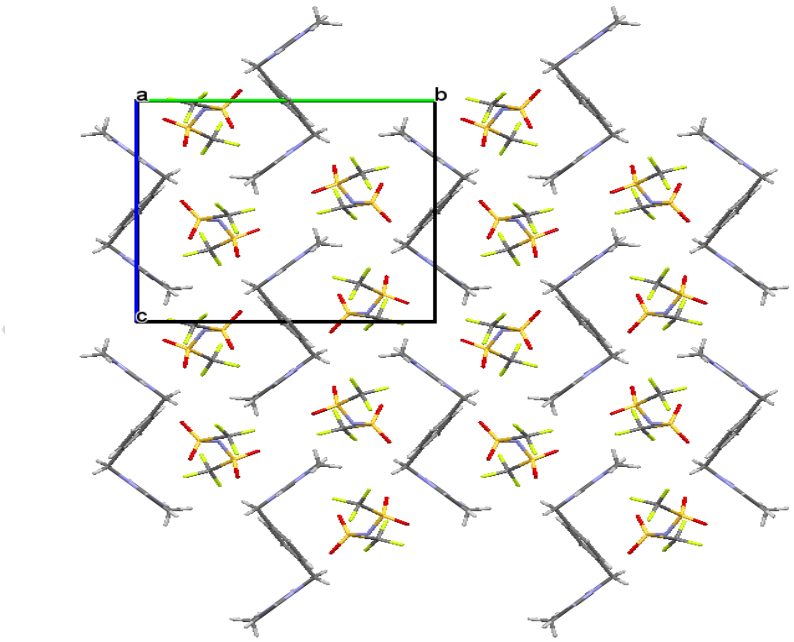

Figure 7. View of crystal packing along the *a* axis for $[p\text{-}C_6H_4(CH_2ImMe)_2^+][(CF_3SO_2)_2N^-]_2$.

4.3 Vibrational spectroscopy measurements and comparison with computational results; detailed FT-Raman and infrared spectroscopy study.

The FT-Raman [45-3300 cm^{-1}] and the IR absorbance [400-3300 cm^{-1}] spectra of the investigated DIL, namely [p-$C_6H_4(CH_2ImMe)_2^+$][$(CF_3SO_2)_2N^-$]$_2$, measured at room temperature are reported in Figures 8. The lines observed as well as their vibrational assignments are summarized in Table 3. Assignments are aided by the DFT calculations and based on a review of the literature assignments performed on related molecules [44-59].

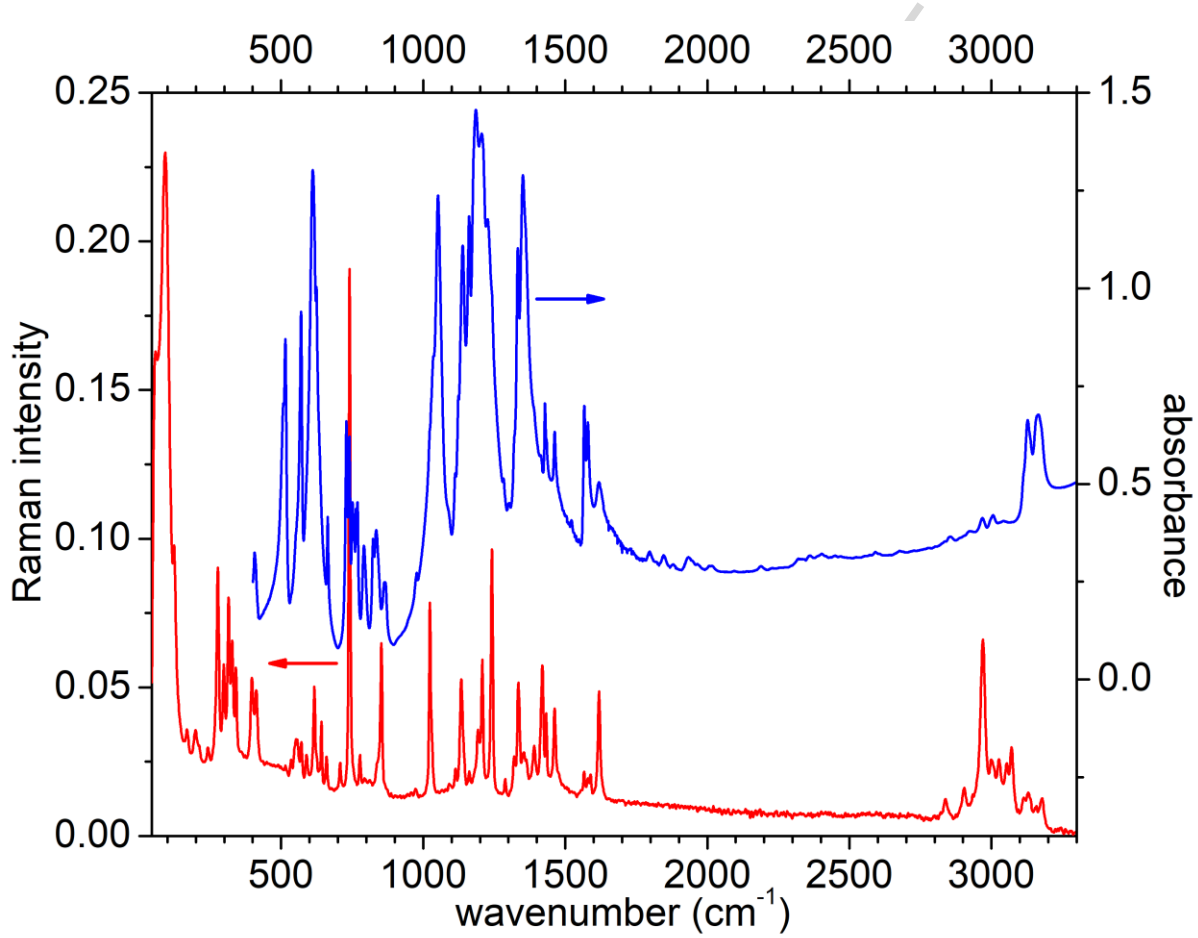

Figure 8. Experimental Raman and infrared vibrational spectra of [p-$C_6H_4(CH_2ImMe)_2^+$][$(CF_3SO_2)_2N^-$]$_2$ in the frequency range 45-3300 cm^{-1}

In the following the comparison of the experimental Raman or infrared spectra with the calculated ones in selected frequency ranges will be presented in order to confirm information about the occurrence of conformers either of the [p-$C_6H_4(CH_2ImMe)_2^+$] cation or of the [$(CF_3SO_2)_2N^-$] anion. The calculated vibration frequency, Raman activity and infrared intensity calculated for the two conformers of the cation are reported in Table S1 of the Supplementing Information, while the same quantities for the conformers of anion have been already reported in the previous literature.[60-61].

Figure 9 reports the experimental Raman spectrum of the compound, compared with the calculated spectra of the two conformers of both anion and cation. Concerning the cation, the absence of the vibration lines centered around 485 and 680 cm^{-1} (marked with the red

asterisks in Fig. 9) indicates the absence of the higher energy conformer (cis geometry), while the spectral marks of the trans geometry of the cation (lines centered around 620, 710 and 783 cm^{-1}) are clearly visible in the experimental Raman spectrum. Concerning the anion, poor information seem to be obtainable from the Raman spectrum. Indeed, the best markers of the presence of the cis or trans conformer of $[(CF_3SO_2)_2N^-]$ are the lines centered around 327 and 340 cm^{-1}, respectively [62]. However, in the present compound a strong Raman band due to the cation is expected around 314 cm^{-1}, and therefore it is not clear whether the experimental band found at 328 cm^{-1} is due to cis-$[(CF_3SO_2)_2N^-]$ or to the cation.

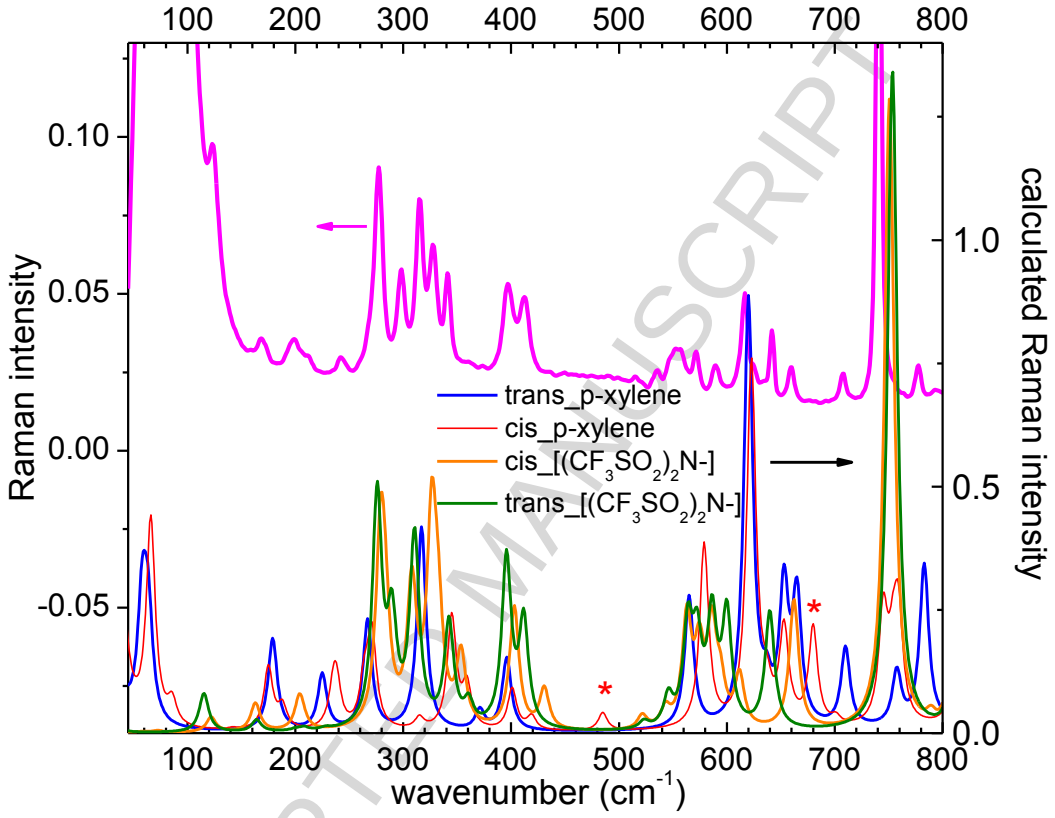

Figure 9. Experimental Raman vibrational spectrum of $[p\text{-}C_6H_4(CH_2ImMe)_2^+][(CF_3SO_2)_2N^-]_2$ in the frequency range 45-500 cm^{-1} (magenta line) and calculated Raman spectra of the two conformers of $[p\text{-}C_6H_4(CH_2ImMe)_2^+]$ and $[(CF_3SO_2)_2N^-]$ (lower part).

Further information can be obtained from the Infrared spectrum, reported in Fig. 10 in the frequency range between 380 and 1000 cm^{-1}, together with the comparison with calculations. Concerning the cation, the absence of the vibration lines centered around 485, 700 and 950 cm^{-1} (marked with the red asterisk in Fig. 10) indicates the absence of the higher energy conformer (cis geometry), while all the spectral marks of the trans geometry of the cation centered between 700 and 900 cm^{-1} are clearly visible in the experimental IR spectrum. Concerning the anion, it is well known that the lines centered around 600 and 650 cm^{-1} are due to the cis conformer (marked in orange in Fig. 10), [34-60] while the single absorption around 620 cm^{-1} is attributable to trans-$[(CF_3SO_2)_2N^-]$. [63-64]. The line at 600 cm^{-1} which could be attributed to the cis conformer is clearly absent in the absorbance spectrum of the presently investigated DIL. A narrow absorption band is visible in the experimental spectrum

around 662 cm^{-1}; its width and position is different from that usually reported for the band due to cis-$[(CF_3SO_2)_2N^-]$ [34,60,63,64], and, therefore, it is more likely due to the trans conformer of the cation.

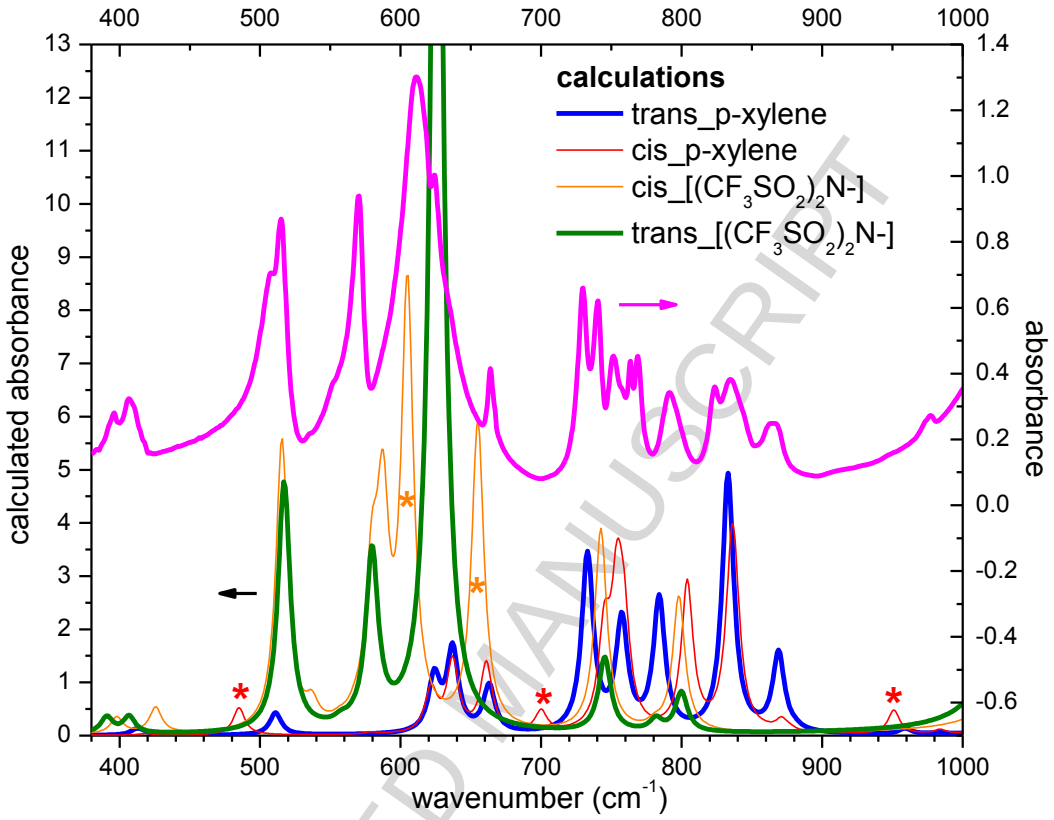

Figure 10. Experimental IR vibrational spectra of $[p\text{-}C_6H_4(CH_2ImMe)_2^+][(CF_3SO_2)_2N^-]_2$ in the frequency range 380-1000 cm^{-1} (magenta line) and calculated IR spectra of the two conformers of $[p\text{-}C_6H_4(CH_2ImMe)_2^+]$ and $[(CF_3SO_2)_2N^-]$ (lower part).

Summing up the vibrational studies, they reveal that in the presently investigated compound only the trans conformer of $[(CF_3SO_2)_2N^-]$ and the trans conformer of the cation are present, in agreement with the results of the XRD measurements.

4.4 Vibrational Band Assignments of $[p\text{-}C_6H_4(CH_2ImMe)_2^+][(CF_3SO_2)_2N^-]_2$

The discussion of assignment of the most important groups for the studied DIL (see Table 3) is presented as follows:

C–H vibrations:

Generally the C-H stretching vibrations give rise to bands in the region of 3200–3000 cm^{-1} in all aromatic compounds, Raman and IR spectra of $[p\text{-}C_6H_4(CH_2ImMe)_2^+][(CF_3SO_2)_2N^-]_2$, were measured over the frequency range 45-3500 cm^{-1} and 400-3500 cm^{-1}. In the range

2700-3500 cm^{-1}, we found several bands originating from both 1-methylimidazole ring, a phenyl ring, and a methylene group. In this region, the C-H bands are affected appreciably by the nature of the substituents and the neighboring group. Accurately, the FT-Raman band observed at 3113, 3128, 3155 and 3177 cm^{-1}, are assigned to Imidazole C–H vibrations, also, the peak positions in the IR spectrum at 3111, 3126, 3163 cm^{-1}, were attributed to the same modes. These stretching frequencies of are similar to those observed by Socrates et al [65]. The similar vibration is computed at 3319, 3299, 3206, 3190, 3174 and 3133 cm^{-1} by DFT with B3LYP/6-31G** basis, in FT-Raman spectrum and at 3319, 3299, 3202, and 3189 cm^{-1} in IR spectrum. In contrast, the CH stretching bands occurring in this region are remarkably weak in the IR spectrum, which is strongly dominated by contributions from the $[(CF_3SO_2)_2N^-]$ anion, and it shows very good correlation with the experimental data.

The methyl group vibrational modes of are observed at 3025, 3052, 3070 cm^{-1} in the FT-Raman spectra, and at 3005 cm^{-1} in IR spectrum. Moreover, the aromatic C–H modes of phenyl rang are observed in the region 2933, 2968, 2999, cm^{-1} in the FT-Raman spectra, and at 2967 in IR spectrum. The bands observed at 2836, 2903 cm^{-1} in FT-Raman spectrum and at 2855 cm^{-1}, in IR spectrum are assigned to the C–H asymmetric and symmetric stretching vibrations in the methylene group. In accordance with the computed wavenumbers these bands are located at 3086 cm^{-1} in IR spectrum and at 3088 cm^{-1} in Raman one.

As reported by Silverstein et al [66], the in-plane C–H bending vibrations appear in the range of 1300–1000 cm^{-1} in the phenyl and the out-of-plane bending vibrations occur in the frequency range of 1000–750 cm^{-1}.

C=C vibrations:

In the present work, C=C stretching bands are observed at 1566, 1579, 1617 cm^{-1} for IR spectrum and at 1565, 1580, 1589 and 1618 cm^{-1} for FT-Raman, The C=C corresponding vibrations appear in DFT calculations at 1491, 1505, 1518, 1601, 1623 cm^{-1}.

C–C and C–N vibrations:

The bands observed at 663 and 729 cm^{-1} in FT-IR are assigned to C-C deformation vibrations of the phenyl ring. The same vibrations in FT-Raman spectrum are at 641, 659, 707 cm^{-1}. The theoretically computed values at 624, 637, 663, and 733 cm^{-1} by the B3LYP/6-311+G(d,p) are in excellent agreement with experimental data.
In addition, both of a C–C stretching and a N-CH_3 twisting are observed at 1051 cm^{-1} [67]. IR spectrum of $[p\text{-}C_6H_4(CH_2ImMe)_2^+]$ and $[(CF_3SO_2)_2N^-]$ shows two bands at 1413, 1428, 1462 cm^{-1}, and at 1418, 1432, 1462 cm^{-1} for FT-Raman one, which may be assigned to the imidazole ring stretching consisting of C–N stretching and in-plane N–C–H bending.
As is seen in Table 3, bands which appears at 1333, 1350 cm^{-1} in the infrared spectrum and at 1319, 1334, 1352, 1364, 1390 cm^{-1} in the FT-Raman spectrum is attributed both to the vibration (C–C) and to the stretching vibration (C-N). In $(N)CH_2$ and $(N)CH_3$, the C–N and

C–C stretching vibrations are observed at 1160, 1184 for IR spectrum and at 1161, 1193 cm^{-1} for FT-Raman, The theoretically calculated values are observed at 1130 and 1176 cm^{-1}.

[$(CF_3SO_2)_2N^-$] anion vibrations:

A number of groups have studied the vibrational spectroscopy of [$(CF_3SO_2)_2N^-$] anion experimentally and computationally [18, 26, 33, 34, 42, 50, 51]. Previous experimental studies based on Raman and infrared spectroscopy, combined with ab-initio or DFT calculations of the vibration frequencies, indicate that this flexible anion can exist in two conformational isomers, cis and trans and all these studies are based on the twisting, wagging and rocking modes of SO_2. In the term of interaction, when Coulombic interactions are predominant, the trans conformer is the most probable, while when the hydrogen bonding or van der Waals interactions become important the cis conformer is favored.
The corresponding FT-Raman and IR spectra are shown in Fig. 6, respectively, which both experimental spectra are presented and predicted also by the DFT calculations.
Based on the existing literature and DFT Calculation, the FT-Raman spectrum is strongly dominated by contributions from the [$(CF_3SO_2)_2N^-$] anion. The Raman modes at 123 and 168 cm^{-1} are assigned to an intramolecular normal mode of [$(CF_3SO_2)_2N^-$] anion, Moreover, the bands observed at 277, 297, 314, 327, 340, 396, 412, 535, 555, 571, 588, 616, 641, 659, 707,741. 1133, 1241, 1334, 1352 cm^{-1} are associated with the vibrations of the [$(CF_3SO_2)_2N^-$] anion. An examination of these bands clearly shows that the mediums bands at 277, 297, 314, 340, 402 and 412 cm^{-1} are associated to the trans-form vibrations.
In IR spectra, the presence of a characteristic band of the trans conformer is observed at 615 cm^{-1}, which indicates that this is the dominant conformation of [$(CF_3SO_2)_2N^-$]. In same Fig. 8 one clearly observes the absence of the IR bands around 600 and 653 cm^{-1}, which are attributed to cis-form. This indicates that the trans conformer is the predominant species in the experimental sample and this is in agreement with our measurement XRD diffraction.
Other bands are also observed at 741, 1051, 1133, 1241, 1334, 1352 cm^{-1} assigned to a CF_3 symmetric stretching (1227 cm^{-1}), and two SO_2 antisymmetric stretching modes.
Our DIL having two [$(CF_3SO_2)_2N^-$] anions and two [p-$C_6H_4(CH_2ImMe)_2^+$] cations in the unit cell. As reported in XRD section, hydrogen bonding between the anion and cation takes place through the methylene group (-CH_2-) and the oxygen atoms of [$(CF_3SO_2)_2N^-$]. Also, between C(2)–H of the imidazole ring and the oxygen atoms of [$(CF_3SO_2)_2N^-$] anion. Thus, these hydrogens bonding with the SO_2 group probably facilitating the adopting of the trans conformation.

Table 3. observed Raman and IR bands of [p-$C_6H_4(CH_2ImMe)_2^+$][$(CF_3SO_2)_2N^-$]$_2$ and their assignment according to the literature or to the present calculations. (vw = very weak, w = weak, m = medium, s = strong, sh = shoulder, Str = stretch, δ = deformation, bend = bending deformation, γ= out the plane deformation, ω = wagging, ρ = rocking, sym = symmetric, asym = antisymmetric).

IR	Raman	vibrational assignment	Refs
	57 (sh)	Intermolecular vibration	[26] /[45] / [46]
	91(s)	Intermolecular vibration	[26] /[45] / [46]
	123(sh)	Intermolecular vibration	[26] /[45] / [46]
	168(vw)	Intermolecular vibration	[26] /[45] / [46]
	198(w)	τ(N–C)/$\rho(CH_2)$, NCH_3	[26]/[27]
	241(vw)	$\rho(CH_2)$, CH_3(N) bend	[25]/[47]
	277(m)/297(w)	$\rho(CH_2)$, CN stretch , Trans-TFSI: ρCF_3,vas(CS)	[46]/ [48]
	314(m)	CN stretch , SC Str Trans-TFSI: $\rho(SO_2)$, $\rho(CF_3)$	[18]/ [46]/ [48]/ [50]
	327(m)	$\rho(SO_2)$,	[18]/ [46]/ [48]/ [50]
	340(m)	δNCH_3, Trans-TFSI: $\tau(SO_2)$	[18]/ [46]/ [48]/ [50]
395(vw)	396 (m)	$\rho(CH_2)$,(N)CH_2 str, Trans-TFSI: $\omega(SO_2)$	[[18]/ [46]/ [48]/ [50]
406(w)	412 (m)	(N)CH_2 str , Trans-TFSI: $\omega(SO_2)$	[18]/ [46]/ [48]/ [50]
507(sh)		$\delta_a CF_3$	[51]
514(s)		$\delta_a CF_3$	[51]
	535 (vw)	Trans-TFSI: δas(CF_3)	[18]/ [46]/ [48]/ [50]
	555 (w)	Trans-TFSI: $\delta s(SO_2)$	[18]/ [46]/ [48]/ [50]
569(s)	571 (w)	Trans-TFSI: δas(CF_3)	[18]/ [46]/ [48]/ [50]
	588 (w)	Trans-TFSI: δas(CF_3), δip as(SO_2), $\delta s(NSO_2)$	[18]/ [46]/ [48]/ [50]
610(s)	616 (m)	Trans-TFSI: δSNS, Phenyl ring νC=C	[18]/ [46]/ [48]/ [50]
623(sh)		CH_3(N) CN Str	[49]
	641 (w)	δCC	[52]-[59]
663(w)	659 (w)	δCC, C=C-H	[52]-[59]
	707 (w)	C=C-H	[52]-[59]
729(m)			
740(m)	741 (s)	Trans TFSI: $\delta s(CF_3)$	[18]/ [46]/ [48]/ [50]
750(w)		ring HCCH sym bend, CF_3 sym bend	[67]
768(w)		ν_sSNS, δ_aHCCH	[51]
	777 (w)	δCC, C=C-H, ring HCCH asym bend	[52]-[59]
790(w)		ring HCCH asym bend	[49]
833(vw)	836 (sh)	ring HCCH asym bend	[52]-[59]
863(vw)	852 (m)	NC(H)N bend,	[18]/ [46]/ [48]/ [50]
976(vw)		CC str, ring ip asym bend	[67]
1034(sh)	1023 (m)	δ CC,	[52]-[59]
1051(s)		Ring ip asym str, CC str,NCH_3 twist, SNS asym str	[67]
1112(sh)	1113 (vw)	δCH, ring HCCH sym bend	[23]
1138(m)	1133 (m)	Trans TFSI: $\nu s(SO_2)$	[28]/[30]
1160(m)	1161 (vw)	δCH,	[28]/[30]
1184(s)	1193 (sh)	Phenyl ring: C–C stretching, C- C-H in plane bending	[52]-[59]
1204(m)	1204 (m)	Phenyl ring: C–C stretching	[52]-[59]
1226(sh)		$\nu_a CF_3$, νCN	[67]
	1241 (m)	Phenyl ring: C–C stretching/ Trans TFSI: $\nu s(CF_3)$	[52]-[59]
1283(sh)	1288 (vw)	Phenyl ring: C–C stretching	[52]-[59]
1301 (vw)		νsCF_3	[67]
	1319 (vw)	Imidazole ring :C–N/ C=N stretching band	[52]-[59]
1333 (m)	1334 (m)	Imidazole ring :C–N/ C=N stretching band/ Trans TFSI: $\nu as(SO_2)$	[52]-[59]
1350 (s)	1352 (vw)	Imidazole ring :C–N/ C=N stretching band, Trans TFSI: $\nu as(SO_2)$,(N)CH_2 str	[52]-[59]
	1364 (sh)	Imidazole ring :C–N/ C=N stretching band, (N)CH_2 str	[52]-[59]
	1390 (w)	Imidazole ring :C–N/ C=N stretching band	[52]-[59]
1413(sh)	1418 (m)	Imidazole ring :C–N / C=N stretching band, (N)CH_2 str, C–H deformation	[52]-[59]
1428 (m)	1432 (w)	Imidazole ring :C–N/ C=N stretching band, δ(CH2), C–H deformation	[52]-[59]
1462 (w)	1462 (m)	Phenyl ring :νC=C, (N)CH_3 str, C–H deformation	[52]-[59]

1520(vw)		Phenyl ring νC=C	[52]-[59]
1566(w)	1565 (vw)	Phenyl ring :νC=C, Imidazole ring ν(N=C)	[52]-[59]
1579(w)	1580 (vw)/1589 (vw)	Phenyl ring :νC=C, (N)CH_2 str	[52]-[59]
1617(w)	1618 (m)	Phenyl ring : νC=C	[52]-[59]
	2836 (w)	(N)CH_2,(N)CH_3 symmetric stretch	[18] / [26]/[27]/[45]/[46]/[51]
2855(vw)		(N)CH_2,(N)CH_3 symmetric stretch	[18]/[26]/[27]/[45]/[46]/[51]
	2903 (w)	(N)CH_2,(N)CH_3 symmetric stretch	[18]/[26]/[27]/[45]/[46]/[51]-[59]
	2933 (vw)	(N)CH_2, (N)CH_3 symmetric stretch	[18]/[26]/[27]/[45]/[46]/[51]-[59]
2967(vw)	2968 (m)	(N)CH_3 asymmetric stretch	[18] /[26]/[27]/[45]/[46]/[51]-[59]
	2999 (w)	(N)CH_3 asymmetric stretch	[18]/[26]/[27]/[45]/[46]/[51]-[59]
3005(vw)			[51]-[59]
	3025 (w)	C-H stretching	[18]/[26]/[27]/[45]/[46]/[51]-[59]
	3052 (w)	C-H stretching, (N)CH_2 str	[18]/[26]/[27]/[45]/[46]/[51]-[59]
	3070 (w)	C-H stretching	[18] / [26]/[27] / [45]/[46] / [51]
3111(sh)	3113 (vw)	H-C-C-H asymmetric stretch	[18]/[26]/[27]/[45]/[46]/[51]-[59]
3126(m)	3128(vw)	H-C-C-H asymmetric stretch	[51]-[59]
	3155 (vw)	H-C-C-H symmetric stretch	[18]/[26]/[27]/[45]/[46]/[51]-[59]
3163(m)		H-C-C-H symmetric stretch	[18]/[26]/[27]/[45]/[46]/[51]-[59]
	3177 (w)	H-C-C-H asymmetric stretch	[18]/[26]/[27]/[45]/[46]/[51]-[59]

5. CONCLUSIONS

The molecular vibrations of new para-xylyl linked di-imidazolium ionic Liquid (DIL) containing the bis(trifluoromethanesulfonyl)imide were investigated by IR and FT-Raman spectroscopies. In addition, density functional method (B3LYP) was used to determine the geometrical and vibrational characteristics of this DIL. In order to determine whether any interactions were present between cation and anion, single crystal X-ray diffraction was employed. The results indicated that all contacts between cation and anion classified as weak hydrogen bonds. Furthermore, the thermal analysis indicated that [p-$C_6H_4(CH_2ImMe)_2^+$][$(CF_3SO_2)_2N^-]_2$ can be classed as ionic liquid since it melts below 100 °C. A comparison of the computational results for the [p-$C_6H_4(CH_2ImMe)_2^+$] cation, the both [$(CF_3SO_2)_2N^-]_2$ anion conformers suggested that only the trans conformer of [$(CF_3SO_2)_2N^-]_2$ and the trans conformer of the [p-$C_6H_4(CH_2ImMe)_2^+$] cation are present, in good agreement with the results of the XRD and IR/FT-Raman measurements.

ACKNOWLEDGEMENTS

The authors gratefully acknowledge the financial support by The Ministry of Higher Education and Scientific Research (MESRS), especially, University of Saïda, Algeria. Moreover, one of the authors (H.Boum.) gratefully acknowledges the efforts of Doctors A-S, M-Dj KHONATI for her support in the experiments section. We would like to thank Quentin Arnould, technician of Walloon Agricultural Research Centre (CRA-W), for assistance with FT-Raman measurements.

REFERENCES

[1] Rogers, R. D., & Seddon, K. R. (2003). Ionic liquids--solvents of the future?. *Science*, *302*(5646), 792-793.
[2] Haddad, B., Mokhtar, D., Goussem, M., Belarbi, E. H., Villemin, D., Bresson, S., ... & Kiefer, J. (2017). Influence of methyl and propyl groups on the vibrational spectra of two imidazolium ionic liquids and their non-ionic precursors. *Journal of Molecular Structure*, *1134*, 582-590.
[3] Salem, N., Zavorine, S., Nucciarone, D., Whitbread, K., Moser, M., & Abu-Lebdeh, Y. (2017). Physical and Electrochemical Properties of Some Phosphonium-Based Ionic Liquids and the Performance of Their Electrolytes in Lithium-Ion Batteries. *Journal of The Electrochemical Society*, *164*(8), H5202-H5209.
[4] Haddad, B., Villemin, D., Belarbi, E. H., Bar, N., & Rahmouni, M. (2014). New dicationic piperidinium hexafluorophosphate ILs, synthesis, characterization and dielectric measurements. *Arabian Journal of Chemistry*, *7*(5), 781-787.
[5] Palumbo, O., Trequattrini, F., Appetecchi, G. B., Conte, L., & Paolone, A. (2017). Relaxation dynamics in pyrrolidinium based ionic liquids: The role of the anion conformers. *Journal of Molecular Liquids*, *243*, 9-13.
[6] Lin, M., Hou, Z. B., Yao, S., Wang, Z. X., & Song, H. (2017). Synthesis and physicochemical properties of new tropine-based chiral dication ionic liquids. *Journal of Molecular Liquids*, *225*, 217-223.
[7] Egorova, K. S., Gordeev, E. G., & Ananikov, V. P. (2017). Biological activity of ionic liquids and their application in pharmaceutics and medicine. *Chem. Rev.*, 2017, 117 (10), 7132–7189.
[8] Sharma, A., Zhang, Y., Gohndrone, T., Oh, S., Brennecke, J. F., McCready, M. J., & Maginn, E. J. (2017). How mixing tetraglyme with the ionic liquid 1-n-hexyl-3-methylimidazolium bis (trifluoromethylsulfonyl) imide changes volumetric and transport properties: An experimental and computational study. *Chemical Engineering Science*, *159*, 43-57.
[9] Depuydt, D., Van den Bossche, A., Dehaen, W., & Binnemans, K. (2017). Metal extraction with a short-chain imidazolium nitrate ionic liquid. *Chemical Communications*, *53*(38), 5271-5274.
[10] García-Garabal, S., Vila, J., Rilo, E., Domínguez-Pérez, M., Segade, L., Tojo, E., ... & Cabeza, O. (2017). Transport properties for 1-ethyl-3-methylimidazolium n-alkyl sulfates: possible evidence of Grotthuss mechanism. *Electrochimica Acta*, *231*, 94-102.
[11] Karpińska, M., Wlazło, M., Zawadzki, M., & Domańska, U. (2018). Liquid-liquid separation of hexane/hex-1-ene and cyclohexane/cyclohexene by dicyanamide-based ionic liquids. *The Journal of Chemical Thermodynamics*, *116*, 299-308.
[12] Bastos, P. D., Oliveira, F. S., Rebelo, L. P., Pereiro, A. B., & Marrucho, I. M. (2015). Separation of azeotropic mixtures using high ionicity ionic liquids based on 1-ethyl-3-methylimidazolium thiocyanate. *Fluid Phase Equilibria*, *389*, 48-54.
[13] Okuniewski, M., Paduszyński, K., & Domańska, U. (2016). Effect of cation structure in trifluoromethanesulfonate-based ionic liquids: density, viscosity, and aqueous biphasic systems involving carbohydrates as "salting-out" agents. *Journal of Chemical & Engineering Data*, *61*(3), 1296-1304.
[14] Sasikumar, Y., Adekunle, A. S., Olasunkanmi, L. O., Bahadur, I., Baskar, R., Kabanda, M. M., ... & Ebenso, E. E. (2015). Experimental, quantum chemical and Monte Carlo simulation studies on the corrosion inhibition of some alkyl imidazolium ionic liquids containing tetrafluoroborate anion on mild steel in acidic medium. *Journal of Molecular Liquids*, *211*, 105-118.
[15] Liew, C. W., & Ramesh, S. (2014). Comparing triflate and hexafluorophosphate anions of ionic liquids in polymer electrolytes for supercapacitor applications. *Materials*, *7*(5), 4019-4033.
[16] Lu, X., Wang, X., Jin, J., Zhang, Q., & Chen, J. (2014). Electrochemical biosensing platform based on amino acid ionic liquid functionalized graphene for ultrasensitive biosensing applications. *Biosensors and Bioelectronics*, *62*, 134-139.
[17] Ji, Y., Hou, Y., Ren, S., Yao, C., & Wu, W. (2018). Highly efficient extraction of phenolic compounds from oil mixtures by trimethylamine-based dicationic ionic liquids via forming deep eutectic solvents. *Fuel Processing Technology*, *171*, 183-191.

[18] Moumene, T., Belarbi, E. H., Haddad, B., Villemin, D., Abbas, O., Khelifa, B., & Bresson, S. (2014). Vibrational spectroscopic study of ionic liquids: Comparison between monocationic and dicationic imidazolium ionic liquids. *Journal of Molecular Structure*, *1065*, 86-92.
[19] Patil, R. A., Talebi, M., Xu, C., Bhawal, S. S., & Armstrong, D. W. (2016). Synthesis of Thermally Stable Geminal Dicationic Ionic Liquids and Related Ionic Compounds: An Examination of Physicochemical Properties by Structural Modification. *Chemistry of Materials*, *28*(12), 4315-4323.
[20] Frizzo, C. P., Gindri, I. M., Bender, C. R., Tier, A. Z., Villetti, M. A., Rodrigues, D. C., ... & Martins, M. A. (2015). Effect on aggregation behavior of long-chain spacers of dicationic imidazolium-based ionic liquids in aqueous solution. *Colloids and Surfaces A: Physicochemical and Engineering Aspects*, *468*, 285-294.
[21] Zhao, D., Liu, M., Zhang, J., Li, J., & Ren, P. (2013). Synthesis, characterization, and properties of imidazole dicationic ionic liquids and their application in esterification. *Chemical engineering journal*, *221*, 99-104.
[22] D'Anna, F., Gunaratne, H. N., Lazzara, G., Noto, R., Rizzo, C., & Seddon, K. R. (2013). Solution and thermal behaviour of novel dicationic imidazolium ionic liquids. *Organic & biomolecular chemistry*, *11*(35), 5836-5846.
[23] Talebi, M., Patil, R. A., Sidisky, L. M., Berthod, A., & Armstrong, D. W. (2017). Branched-chain dicationic ionic liquids for fatty acid methyl ester assessment by gas chromatography. *Analytical and bioanalytical chemistry*, 1-11.
[24] Verma, P. L., Bartolotti, L. J., & Gejji, S. P. (2016). Probing Molecular Interactions in Functionalized Asymmetric Quaternary Ammonium-Based Dicationic Ionic Liquids. *The Journal of Physical Chemistry A*, *120*(39), 7732-7744.
[25] Shirota, H., & Ishida, T. (2011). Microscopic Aspects in Dicationic Ionic Liquids through the Low-Frequency Spectra by Femtosecond Raman-Induced Kerr Effect Spectroscopy. *The Journal of Physical Chemistry B*, *115*(37), 10860-10870.
[26] Moumene, T., Belarbi, E. H., Haddad, B., Villemin, D., Abbas, O., Khelifa, B., & Bresson, S. (2015). Study of imidazolium dicationic ionic liquids by Raman and FTIR spectroscopies: The effect of the nature of the anion. *Journal of Molecular Structure*, *1083*, 179-186.
[27] Kadari, M., Belarbi, E. H., Moumene, T., Bresson, S., Haddad, B., Abbas, O., & Khelifa, B. (2017). Comparative study between 1-Propyl-3-methylimidazolium bromide and trimethylene bis-methylimidazolium bromide ionic liquids by FTIR/ATR and FT-RAMAN spectroscopies. *Journal of Molecular Structure*, *1143*, 91-99.
[28] Chen, W., Wu, B., & Matsumoto, K. (2002). Synthesis and crystal structure of N-heterocyclic carbene complex of silver. *Journal of organometallic chemistry*, *654*(1), 233-236.
[29] Baker, M. V., Brown, D. H., Haque, R. A., Skelton, B. W., & White, A. H. (2009). Silver (I) and mercury (II) complexes of meta-and para-xylyl linked bis (imidazol-2-ylidenes). *Journal of Inclusion Phenomena and Macrocyclic Chemistry*, *65*(1-2), 97-109.
[30] Sheldrick, G. M. (1990). SHELXS 97, Program for Crystal Structure Refinement, University of Göttingen, Germany, 1997 Search PubMed;(b) P. van der Sluis and AL Spek. *Acta Crystallogr., Sect. A: Found. Crystallogr*, *46*, 194.
[31] Sheldrick, G. M. (2014). SHELXL-2014/7: Program for the Solution of Crystal Structures. University of Göttingen, Göttingen, Germany.

[32] Shao, Y., Molnar, L. F., Jung, Y., Kussmann, J., Ochsenfeld, C., Brown, S. T., ... & Gill, P.M.W., and Head-Gordon, M., (2006). Advances in methods and algorithms in a modern quantum chemistry program package. *Physical Chemistry Chemical Physics*, *8*(27), 3172-3191.
[33] Hehre, W. J. (2003). *A guide to molecular mechanics and quantum chemical calculations* (Vol. 2). Irvine, CA: Wavefunction.
[34] Paschoal, V. H., Faria, L. F., & Ribeiro, M. C. (2017). Vibrational Spectroscopy of Ionic Liquids. *Chemical reviews*, *117*(10), 7053-7112.
[35] Capitani, F., Trequattrini, F., Palumbo, O., Paolone, A., & Postorino, P. (2016). Phase transitions of PYR14-TFSI as a function of pressure and temperature: the competition between smaller volume and lower energy conformer. *The Journal of Physical Chemistry B*, *120*(11), 2921-2928.

[36] Vitucci, F. M., Trequattrini, F., Palumbo, O., Brubach, J. B., Roy, P., Navarra, M. A., ... & Paolone, A. (2014). Stabilization of different conformers of bis (trifluoromethanesulfonyl) imide anion in ammonium-based ionic liquids at low temperatures. *The Journal of Physical Chemistry A*, *118*(38), 8758-8764.
[37] Marsh, K. N., Boxall, J. A., & Lichtenthaler, R. (2004). Room temperature ionic liquids and their mixtures—a review. *Fluid Phase Equilibria*, *219*(1), 93-98.
[38] Ibrahim, H., Koorbanally, N. A., Ramjugernath, D., Bala, M. D., & Nyamori, V. O. (2012). Synthesis and characterization of imidazolium salts bearing fluorinated anions. *Zeitschrift für anorganische und allgemeine Chemie*, *638*(14), 2304-2309.
[39] Weingärtner, H. (2008). Understanding ionic liquids at the molecular level: facts, problems, and controversies. *Angewandte Chemie International Edition*, *47*(4), 654-670.
[40] Wilkes, J. S. (2002). A short history of ionic liquids—from molten salts to neoteric solvents. *Green Chemistry*, *4*(2), 73-80.
[41] Willans, C. E., Anderson, K. M., Paterson, M. J., Junk, P. C., Barbour, L. J., & Steed, J. W. (2009). Bis (N- heterocyclic carbene) Dipalladium Complexes: Synthesis, Solid- State Conformational Studies and Solution Behaviour. *European Journal of Inorganic Chemistry*, *2009*(19), 2835-2843.
[42] Holbrey, J. D., Reichert, W. M., & Rogers, R. D. (2004). Crystal structures of imidazolium bis (trifluoromethanesulfonyl) imide 'ionic liquid'salts: the first organic salt with a cis-TFSI anion conformation. *Dalton Transactions*, (15), 2267-2271.
[43] Levason, W., Pugh, D., & Reid, G. (2017). Imidazolium-based ionic liquids with large weakly coordinating anions. *New Journal of Chemistry*, *41*(4), 1677-1686.
[44] Panda, S., Kundu, K., Umapathy, S., & Gardas, R. L. (2017). A Combined Experimental and Theoretical Approach to Understand the Structure and Properties of N- Methylpyrrolidone- Based Protic Ionic Liquids. *ChemPhysChem*, *18(23)*, 3416–3428.
[45] Moumene, T., Belarbi, E. H., Haddad, B., Villemin, D., Abbas, O., Khelifa, B., & Bresson, S. (2015). Study of imidazolium dicationic ionic liquids by Raman and FTIR spectroscopies: The effect of the nature of the anion. *Journal of Molecular Structure*, *1083*, 179-186.
[46] Drai, M., Mostefai, A., Paolone, A., Haddad, B., Belarbi, E., Villemin, D., ... & Rahmouni, M. (2017). Synthesis, experimental and theoretical vibrational studies of 1-methyl and 1, 2-dimethyl, 3-propyl imidazolium bis (trifluoromethanesulfonyl) imide. *Journal of Chemical Sciences*, *129*(6), 707-719.
[47] Heimer, N. E., Del Sesto, R. E., Meng, Z., Wilkes, J. S., & Carper, W. R. (2006). Vibrational spectra of imidazolium tetrafluoroborate ionic liquids. *Journal of molecular liquids*, *124*(1), 84-95.
[48] Talaty, E. R., Raja, S., Storhaug, V. J., Dölle, A., & Carper, W. R. (2004). Raman and infrared spectra and ab initio calculations of C2-4MIM imidazolium hexafluorophosphate ionic liquids. *The Journal of Physical Chemistry B*, *108*(35), 13177-13184.
[49] Chaker, Y., Ilikti, H., Debdab, M., Moumene, T., Belarbi, E. H., Wadouachi, A., ... & Bresson, S. (2016). Synthesis and characterization of 1-(hydroxyethyl)-3-methylimidazolium sulfate and chloride ionic liquids. *Journal of Molecular Structure*, *1113*, 182-190.
[50] Haddad, B., Paolone, A., Villemin, D., Taqiyeddine, M., Belarbi, E. H., Bresson, S., ... & Kiefer, J. (2017). Synthesis, conductivity, and vibrational spectroscopy of tetraphenylphosphonium bis (trifluoromethanesulfonyl) imide. *Journal of Molecular Structure*, 1146, 203-212
[51] Moschovi, A. M., Ntais, S., Dracopoulos, V., & Nikolakis, V. (2012). Vibrational spectroscopic study of the protic ionic liquid 1-H-3-methylimidazolium bis (trifluoromethanesulfonyl) imide. *Vibrational Spectroscopy*, *63*, 350-359.
[52] Güllüoğlu, M. T., Erdogdu, Y., Karpagam, J., Sundaraganesan, N., & Yurdakul, Ş. (2011). DFT, FT-Raman, FT-IR and FT-NMR studies of 4-phenylimidazole. *Journal of Molecular Structure*, *990*(1), 14-20.
[53] Sudha, S., Karabacak, M., Kurt, M., Cinar, M., & Sundaraganesan, N. (2011). Molecular structure, vibrational spectroscopic, first-order hyperpolarizability and HOMO, LUMO studies of 2-aminobenzimidazole. *Spectrochimica Acta Part A: Molecular and Biomolecular Spectroscopy*, *84*(1), 184-195.

[55] Cui, S., Wang, T., & Hu, X. (2014). Synthesis, characterization, and DFT studies of a new chiral ionic liquid from (S)-1-phenylethylamine. *Spectrochimica Acta Part A: Molecular and Biomolecular Spectroscopy*, *133*, 778-784.
[56] Erdogdu, Y., Güllüoğlu, M. T., Yurdakul, S., & Dereli, Ö. (2012). DFT simulations, FT-IR, FT-raman, and FT-NMR spectra of 4-(4-chlorophenyl)-1H-imidazole molecules. *Optics and Spectroscopy*, *113*(1), 23-32.
[57] Malek, K., Puc, A., Schroeder, G., Rybachenko, V. I., & Proniewicz, L. M. (2006). FT-IR and FT-Raman spectroscopies and DFT modelling of benzimidazolium salts. *Chemical physics*, *327*(2), 439-451.
[58] Hommel, E. L., & Allen, H. C. (2003). The air–liquid interface of benzene, toluene, m-xylene, and mesitylene: a sum frequency, Raman, and infrared spectroscopic study. *Analyst*, *128*(6), 750-755.
[59] Sharma, S. K., Misra, A. K., & Sharma, B. (2005). Portable remote Raman system for monitoring hydrocarbon, gas hydrates and explosives in the environment. *Spectrochimica Acta Part A: Molecular and Biomolecular Spectroscopy*, *61*(10), 2404-2412.
[60] Vitucci, F. M., Trequattrini, F., Palumbo, O., Brubach, J. B., Roy, P., & Paolone, A. (2014). Infrared spectra of bis (trifluoromethanesulfonyl) imide based ionic liquids: Experiments and DFT simulations. *Vibrational Spectroscopy*, *74*, 81-87.
[61] Herstedt, M., Smirnov, M., Johansson, P., Chami, M., Grondin, J., Servant, L., & Lassegues, J. C. (2005). Spectroscopic characterization of the conformational states of the bis (trifluoromethanesulfonyl) imide anion (TFSI−). *Journal of Raman Spectroscopy*, *36*(8), 762-770.
[62] Capitani, F., Trequattrini, F., Palumbo, O., Paolone, A., & Postorino, P. (2016). Phase transitions of PYR14-TFSI as a function of pressure and temperature: the competition between smaller volume and lower energy conformer. *The Journal of Physical Chemistry B*, *120*(11), 2921-2928.
[63] Palumbo, O., Trequattrini, F., Appetecchi, G. B., & Paolone, A. (2017). Influence of Alkyl Chain Length on Microscopic Configurations of the Anion in the Crystalline Phases of PYR1A-TFSI. *The Journal of Physical Chemistry C*.
[64] Palumbo, O., Trequattrini, F., Navarra, M. A., Brubach, J. B., Roy, P., & Paolone, A. (2017). Tailoring the physical properties of the mixtures of ionic liquids: a microscopic point of view. *Physical Chemistry Chemical Physics*, *19*(12), 8322-8329.
[65] Socrates, G. (2001). *Infrared and Raman characteristic group frequencies: tables and charts*. John Wiley & Sons.
[66] Silverstein, R. M., Webster, F. X., Kiemle, D. J., & Bryce, D. L. (2014). *Spectrometric identification of organic compounds*. John wiley & sons.
[67] Kiefer, J., Fries, J., & Leipertz, A. (2007). Experimental vibrational study of imidazolium-based ionic liquids: Raman and infrared spectra of 1-ethyl-3-methylimidazolium bis (trifluoromethylsulfonyl) imide and 1-ethyl-3-methylimidazolium ethylsulfate. *Applied spectroscopy*, *61*(12), 1306-1311.

Graphical Abstract.

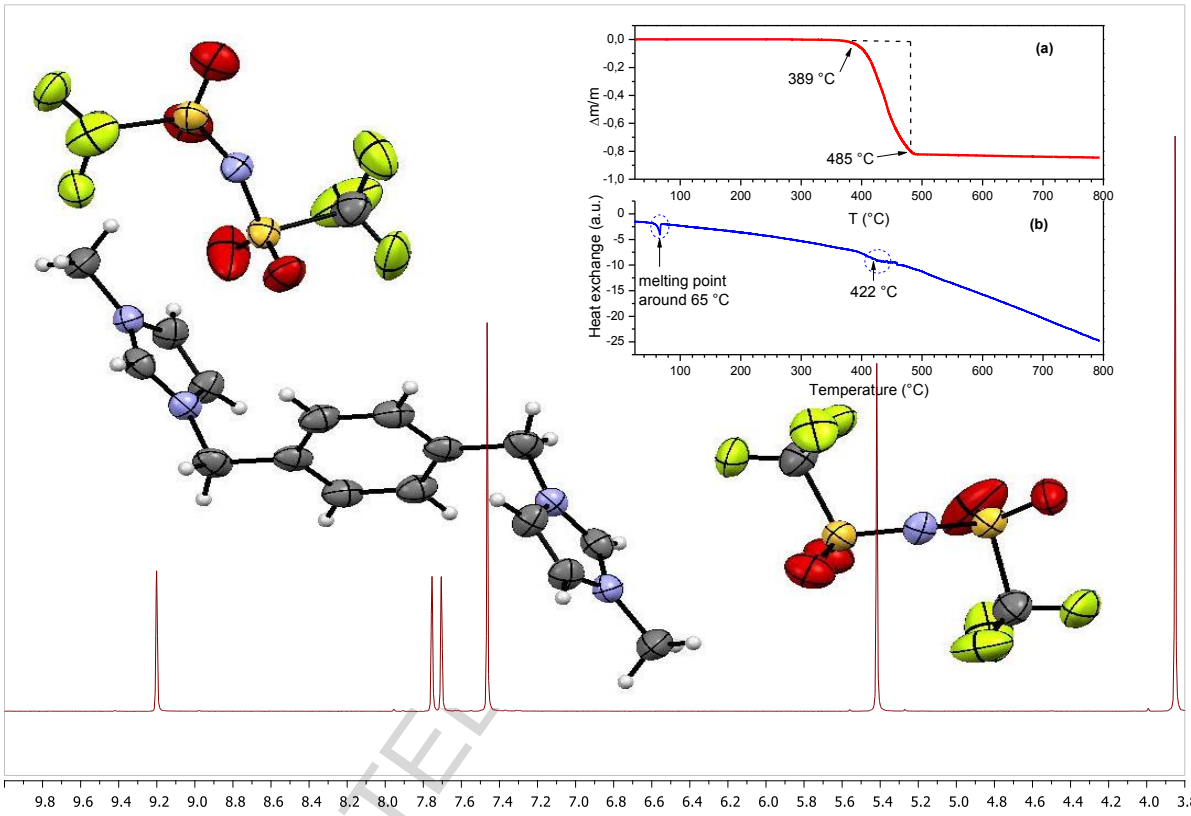

Highlights

1) Synthesis and crystal structure of [p-$C_6H_4(CH_2ImMe)_2^+$][$(CF_3SO_2)_2N^-$]$_2$.

2) Thermal stability of [p-$C_6H_4(CH_2ImMe)_2^+$][$(CF_3SO_2)_2N^-$]$_2$.

3) Only the Trans conformers of both cation and anion are present.

4) Interaction between [p-$C_6H_4(CH_2ImMe)_2$] and [$(CF_3SO_2)_2N^-$].